universe

MDPI

Article

Hartree–Fock Calculations in Semi-Infinite Matter with Gogny Interactions

Dany Davesne [1,*,†], Alessandro Pastore [2,†] and Jesus Navarro [3,†]

[1] Institut de Physique des 2 Infinis de Lyon, CNRS-IN2P3, Université Lyon 1, 43 Bd. du 11 Novembre 1918, CEDEX, F-69622 Villeurbanne, France
[2] CEA, DES, IRESNE, DER, SPRC, F-13108 Saint Paul Lez Durance, France; alessandro.pastore@cea.fr
[3] Instituto de Física Corpuscular (CSIC-Universidad de Valencia), Apartado Postal 22085, E-46.071 Valencia, Spain; navarro@ific.uv.es
* Correspondence: davesne@ipnl.in2p3.fr
† These authors contributed equally to this work.

Abstract: Hartree–Fock equations in semi-infinite nuclear matter for finite range Gogny interactions are presented together with a detailed numerical scheme to solve them. The value of the surface energy is then extracted and given for standard Gogny interactions.

Keywords: Nuclear Density Functional Theory; semi-infinite nuclear matter; Hartree–Fock equations

PACS: 21.60.Jz; 21.65.-f; 21.65.Mn

1. Introduction

The liquid drop model [1] describes the isotopic dependence of the nuclear binding energy in terms of only five adjustable coupling constants, each of them with a simple physical interpretation [2]. Furthermore, by considering a system with an equal number of neutrons and protons and neglecting electromagnetic and pairing effects [3], the binding energy simply consists of a balance between volume and surface terms. Despite the atomic nucleus being a very complex many-body system, the droplet interpretation provides us with a unique insight into basic nuclear phenomena such as fusion or fission.

Instead of describing the nucleus as a droplet, it is, however, realistic to adopt a more microscopic approach by using mean field methods [4]. By solving the self-consistent Hartree–Fock (HF) equations using an effective nucleon-nucleon interaction plus BCS [1] to take into account superfluid effects, one can describe a large variety of nuclear observables such as masses or radii [5] with great accuracy [6] without assuming any a priori shape of the system. The quality of the HF calculations strongly depends on the properties of the underlying effective interaction used. Within the scientific literature, one finds a large variety of them, but limiting ourselves to the non-relativistic case, we can clearly identify two major families: the zero-range Skyrme interaction [7] and the finite-range ones such as Gogny [8] and Nakada [9].

These interactions are characterised by a small set of adjustable coupling constants, typically about ten [10], that are constrained during a fitting procedure [11]. There is no global consensus on the pool of observables used in the optimisation procedure of the coupling constants, but it is quite a common practice to perform the fit using infinite nuclear matter (INM) properties in order to constrain the volume part and finite nuclei properties to properly take into account surface and finite size effects. As an example, we refer the reader to Refs. [12,13], where two different protocols have been implemented in order to adjust the coupling constants of the effective interactions.

Several articles have highlighted the strong correlation between the surface energy associated with an effective interaction and deformation properties, with particular attention

check for updates

Citation: Davesne, D.; Pastore, A.; Navarro, J. Hartree–Fock Calculations in Semi-Infinite Matter with Gogny Interactions. *Universe* **2023**, *9*, 398. https://doi.org/10.3390/universe9090398

Academic Editors: Maria Benedetta Barbaro, Marco Martini and Arturo De Pace

Received: 30 June 2023
Revised: 1 August 2023
Accepted: 28 August 2023
Published: 30 August 2023

to fission (see, for example, Refs. [14,15] and references therein). In particular, it has been shown that with a surface energy coefficient $a_s \approx 18$ MeV, the resulting interaction is capable of reproducing reasonably well deformation properties and fission barrier of some selected nuclei. Exploiting such a correlation during a fitting procedure is very important since instead of calculating the properties of a deformed nucleus or a fission barrier, which are quite computationally expensive, one can calculate the surface energy in a simpler system such as semi-infinite nuclear matter (SINM), eventually using some semi-classical approximation [14]. Our aim is to study some relevant Gogny parametrisations and examine the differences between the HF value of the surface energy and the semi-classical one as in the recent article [16]. The aim of the present article is a first step in that direction and represents an extension of the pioneering work of Côté and Pearson [17] in SINM. In this paper, we present a new numerical HF solver for SINM and the associated numerical procedure capable of handling the most recent Gogny parametrisations.

The article is organised as follows: in Section 2.1, we briefly discuss the properties of infinite nuclear matter of a few selected Gogny interactions; in Section 2.2, we present the formalism of the Hartree–Fock equations in SINM, while in Section 3, we present our results. The conclusions are drawn in Section 4.

2. Materials and Methods

2.1. Infinite Nuclear Matter

INM is an ideal homogeneous system where finite size effects and Coulomb interactions are neglected. The system is infinite along all directions and characterised solely by the neutron and proton densities ρ_n and ρ_p. By varying the asymmetry parameter $\beta \equiv \frac{\rho_n - \rho_p}{\rho}$ with $\rho = \rho_n + \rho_p$, we can go from symmetric nuclear matter to a system made only of pure neutron matter. Note that in the following, we will always consider spin-saturated systems since they are sufficient to cover our goal. Despite being ideal, INM is, however, very interesting since several quantities of interest, such as the energy per particle, can be calculated using various many-body methods and thus offer a unique opportunity to compare various techniques. Moreover, INM can also be used in practice to describe physical objects such as neutron stars [18]. In the following section, we will restrain ourselves to a mean field description of the system using an effective Gogny interaction of the form.

$$V(\mathbf{r}_1, \mathbf{r}_2) = V_C(\mathbf{r}_1, \mathbf{r}_2) + V_{DD}(\mathbf{r}_1, \mathbf{r}_2) + V_{SO}(\mathbf{r}_1, \mathbf{r}_2), \tag{1}$$

where the various terms read

$$V_C(\mathbf{r}_1, \mathbf{r}_2) = \sum_i (W_i + B_i P_\sigma - H_i P_\tau - M_i P_\sigma P_\tau) e^{-r_{12}^2/\mu_i^2} \tag{2}$$

$$V_{DD}(\mathbf{r}_1, \mathbf{r}_2) = t_3 (1 + x_3 P_\sigma) \rho^\gamma \delta(\mathbf{r}_{12}) \tag{3}$$

$$V_{SO}(\mathbf{r}_1, \mathbf{r}_2) = i W_0 (\mathbf{k}' \times \mathbf{k}) (\sigma_1 + \sigma_2) \delta(\mathbf{r}_{12}) \tag{4}$$

where P_σ, P_τ are the spin/isospin exchange operators, $\mathbf{r}_{12} = \mathbf{r}_1 - \mathbf{r}_2$, $\mathbf{k} = -\frac{i}{2}(\nabla_1 - \nabla_2)$ is the relative momentum operator acting on the right and $\mathbf{k}'$ its conjugate acting on the left, and σ_i are the Pauli matrices. See Refs. [10,19] for more details. The density-dependent term, $V_{DD}(\mathbf{r}_1, \mathbf{r}_2)$, and the spin-orbit one, $V_{SO}(\mathbf{r}_1, \mathbf{r}_2)$, have the same form as in the Skyrme interaction both being zero-range [7]. A second density-dependent term of the form $V_{DDb}(\mathbf{r}_1, \mathbf{r}_2) = t_{3b}(1 + x_{3b} P_\sigma) \rho^{\gamma_b} \delta(\mathbf{r}_{12})$ has been considered for the D1P parametrisation [20] in order to gain more flexibility in the fitting procedure. Within the scientific literature, some non-trivial extensions of the Gogny interaction have also been suggested: for example, D1ST2A [21] and GT2 [22] include an explicit tensor term or the more recent D2 [23] parametrisation that replaces the zero-range density-dependent term by a finite-range one. For sake of simplicity, we investigate in the current article the surface properties of various Gogny parametrisations of the *standard* form given in Equation (1) only.

Given the interaction, it is then possible to derive INM properties. In Figure 1, we show by instance the energy per particle (E/A) in symmetric nuclear matter for the standard Gogny interactions considered here. As expected, all of them produce a very similar equation of state on a large density range.

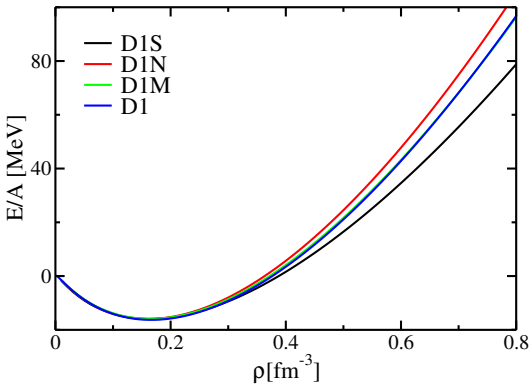

Figure 1. (Color online) Energy per particle in symmetric nuclear matter as a function of the density for various standard Gogny interactions.

In Table 1, we also provide a summary of some other INM properties, such as the energy per particle at saturation density, the saturation density, the isoscalar effective mass m^*/m, the symmetry energy J and its first derivative L. We notice that all these interactions give very similar values for the effective mass and symmetry energy, while they differ on their slope L.

The original D1 interaction [8] was developed and used for systematic calculations in finite nuclei. However, in Ref. [24], the authors showed that D1 was not suitable for the description of properties of fissile nuclei such as ^{240}Pu. For such a reason, a new interaction, named D1S [8], was suggested. D1S has been since widely used for nuclear structure calculations; however, from Table 1, one sees that some bulk properties are still not fully satisfactory as for example the very small value of L clearly incompatible with the values currently adopted in the literature [25] and arising from various experimental measurements such as neutron skins of heavy nuclei or neutron star properties [26–29]. In order to mitigate the poor description of neutron-rich nuclei of D1S, a new interaction D1N has been developed [30], showing that it was possible to provide a good reproduction of both INM and finite nuclei properties using this type of finite range interaction. The D1M [31] interaction has finally been fitted in this spirit by trying to further improve the description of finite nuclei by taking explicitly into account some effects beyond mean field level [32]. At the present time, this is the only effective finite-range interaction that can be used to produce a large-scale calculation of nuclear binding energies with an average discrepancy, compared to experiment, of less than 1 MeV [33].

The study of INM properties gives us precious information about the bulk properties of the nuclear interaction, but in order to have an insight into surface properties, we need to move to the SINM, as discussed in the next section.

Table 1. INM properties of selected Gogny interactions. See text for details.

	E/A(ρ_0) [MeV]	**ρ_0 [fm^{-3}]**	**m^*/m**	**J [MeV]**	**L [MeV]**
D1 [8]	−16.30	0.166	0.670	30.70	18.36
D1S [8]	−16.01	0.163	0.697	31.13	22.43
D1N [30]	−15.94	0.161	0.657	29.58	33.58
D1M [31]	−15.92	0.165	0.749	28.55	24.75

2.2. Semi Infinite Nuclear Matter

Following the original work of Swiatecki [34], we define SINM as an infinite medium along two directions, say x, y in cartesian coordinates, and with a well-defined surface along the z-axis. Along this direction, the matter density ρ varies between two asymptotic values:

$$\lim_{z\to\pm\infty} \rho(z) = \begin{cases} \rho_0\,, \\ 0\,. \end{cases} \tag{5}$$

Since the system is infinite along z, the above asymptotic value ρ_0 is not impacted by the presence of a surface around $z = 0$ and is thus set to the standard INM value.

In Figure 2, we illustrate the results of various Hartree–Fock calculations in SINM using the selected Gogny interactions. In this article, we provide a general formalism to study SINM at any value of isospin asymmetry, but for the moment, we will present numerical results only for systems with an equal number of neutrons and protons, i.e., $\beta = 0$.

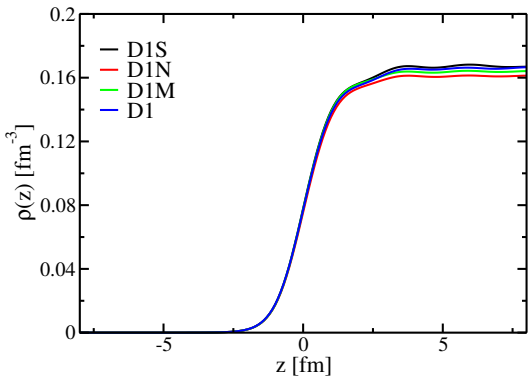

Figure 2. Total density profile for various Gogny interactions calculated in SINM at $\beta = 0$. See text for details.

We observe that the density does not fall abruptly at $z = 0$ but exhibits a diffusivity directly linked to the chosen interaction. We also notice that the density in the matter side is not totally flat but presents the so-called Friedel oscillations [35] that persist over a large range of z. Since these oscillations are only very slowly damped, they may impact the estimate of the surface energy. This problem has been extensively discussed in Ref. [14], and we will briefly return to it in Section 3.2. Since the selected Gogny interactions have different saturation densities, as shown in Table 1, we observe that the asymptotic value of $\rho(z)$ is different when approaching the edge of the box.

In order to perform our study, we follow the procedure detailed in Ref. [17] i.e., we consider a slab of this medium with a unit cross section in the (x, y) plane and extending between $[-L, L]$ in the z-direction. The total energy of such a system reads

$$E_L = \int_{-L}^{L} \mathcal{E}(z)dz, \tag{6}$$

where $\mathcal{E}(z)$ is the energy density. We then calculate the same quantity over the same range, but considering that we have INM in the whole range. In that case, we obtain

$$E'_L = a_v \int_{-L}^{L} \rho(z)dz, \tag{7}$$

where $a_v = \mathrm{E/A}(\rho_0)$ is the energy per particle of INM. By definition, the difference between these two quantities represents the surface energy per unit area

$$\sigma = \lim_{L\to\infty} \int_{-L}^{L} (\mathcal{E}(z) - a_v\rho(z))dz \tag{8}$$

which can be converted into the surface energy per nucleon as

$$a_s = \left(\frac{36\pi}{\rho_0^2}\right)^{\frac{1}{3}} \sigma. \tag{9}$$

The above considerations are quite general, and the use of a specific approach (Hartree–Fock, Thomas–Fermi, ...) is now required to calculate explicitly $\mathcal{E}(z)$ and $\rho(z)$. We proceed now to discuss the Hartree–Fock equations, which is the approach used in the present work. Assuming that the wavefunction of the system can be described as a Slater determinant, the HF equations for SINM can be easily obtained. They read

$$\left\{-\frac{\hbar^2}{2m}\nabla^2 + U(z,k_z,k_t) + U_q^{SO}(z)(\mathbf{k}\times\boldsymbol{\sigma})_z\right\}\phi_\mu(\mathbf{r}) = \varepsilon_\mu(\mathbf{r})\phi_\mu(\mathbf{r}) \tag{10}$$

where μ is a generic index that stands for the quantum numbers of the system. At this stage, in order to simplify the notation, we neglect the isospin dependence. Since the system is infinite and homogeneous in the x, y plane, it is convenient to use a mixed representation of the wavefunction in coordinate and momentum spaces. Following Ref. [36], we write it as

$$\phi_\mu(\mathbf{r}) = \sqrt{2}\psi_\lambda(z,k_z,k_t)\chi_\lambda(\hat{\mathbf{k}}_t)e^{i\mathbf{k}_t\cdot\mathbf{r}} \tag{11}$$

where $\mathbf{k}_t$ is the transverse momentum (with respect to the surface). As discussed in Ref. [17] the spinor $\chi_\lambda(\hat{\mathbf{k}}_t)$ is an eigenvector of $(\mathbf{k}\times\boldsymbol{\sigma})_z$ with eigenstates $\lambda = \pm 1$. Injecting Equation (11) in Equation (10), we obtain

$$\left(-\frac{\hbar^2}{2m}\frac{d^2}{dz^2} + U_q^0(z) + \lambda k_t U_q^{SO}(z) - \varepsilon_q(k_z,k_t) + \frac{\hbar^2 k_t^2}{2m}\right)\psi_{q\lambda}(z,k_z,k_t) = \int_{-\infty}^{\infty} U_q^1(z,z',k_t,k_z)\psi_{q\lambda}(z',k_z,k_t)dz' \,, \tag{12}$$

where U_q^0, U_q^1, U_q^{SO} represent the Hartree, Fock and spin-orbit contributions and q is an index that stands for neutrons and protons. For a standard Gogny interaction considered here, these fields read

$$\begin{aligned}
U_q^0(z) &= \frac{\pi}{2}\sum_i \mu_i^2 \int_{-\infty}^{\infty}\left[(2W_i+B_i)\rho(z') - (2H_i+M_i)\rho_q(z')\right]e^{-(z-z')^2/\mu_i^2}dz' - \frac{W_0}{2}\frac{d}{dz}\left(J(z)+J_q(z)\right) \\
&+ t_3\rho^\alpha(z)\left[\left(1+\frac{x_3}{2}\right)\rho(z) - \left(\frac{1}{2}+x_3\right)\rho_q(z)\right] + \frac{t_3}{8}\alpha\rho^{\alpha+1}(z)\left[3-(2x_3+1)\beta^2\right] \\
&+ t_3\rho^\alpha(z)\left[\left(1+\frac{x_3}{2}\right)\rho(z) - \left(\frac{1}{2}+x_3\right)\rho_q(z)\right] \\
&+ \frac{t_3}{2}\alpha\rho^{\alpha-1}(z)\left[\left(1+\frac{x_3}{2}\right)\rho^2(z) - \left(\frac{1}{2}+x_3\right)\sum_{q'}\rho_{q'}^2(z)\right],
\end{aligned} \tag{13}$$

$$\begin{aligned}
U_q^1(z,z',k_t,k_z) &= \frac{1}{2\pi}\sum_i\sum_{q'}\sum_\lambda \mu_i^2 e^{-(z-z')^2/\mu_i^2}\left[(2M_i+H_i) - (2B_i+W_i)\delta_{qq'}\right] \\
&\times \int_0^{k_{Fq}}\int_0^{\sqrt{k_{Fq}^2-k_z'^2}} k_t'\psi_{q'\lambda}^*(z,k_z',k_t')\psi_{q'\lambda}(z',k_z',k_t')e^{-\mu_i^2(k_t^2+k_t'^2)/4}I_0\left(\frac{\mu_i^2 k_t k_t'}{2}\right)dk_t'dk_z',
\end{aligned} \tag{14}$$

$$U_q^{SO}(z) = \frac{1}{2}W_0\left(\nabla\rho(z) + \nabla\rho_q(z)\right). \tag{15}$$

where $k_{Fq} = (3\pi^2\rho_q)^{1/3}$ represents the Fermi momentum of each species and $I_0(x)$ is the modified Bessel function of zeroth order [37]. Moreover, the explicit expressions of the local matter density and spin-current density entering the above equations are

$$\rho_q(z) = \frac{1}{\pi^2}\sum_\lambda \int_0^{k_{Fq}} \int_0^{\sqrt{k_{Fq}^2-k_z^2}} |\psi_{q\lambda}(z,k_z,k_t)|^2 k_t dk_t dk_z \quad (16)$$

$$J(z) = \frac{1}{\pi^2}\sum_\lambda \lambda \int_0^{k_{Fq}} \int_0^{\sqrt{k_{Fq}^2-k_z^2}} |\psi_{q\lambda}(z,k_z,k_t)|^2 k_t^2 dk_t dk_z \quad (17)$$

It is important to notice that $J(z)$ is only non-zero along the z direction and vanishes when the spin-orbit interaction is set to zero. In order to calculate the total energy, we will also make use of the kinetic energy density

$$\tau_q(z) = \frac{1}{\pi^2}\sum_\lambda \int_0^{k_{Fq}} \int_0^{\sqrt{k_{Fq}^2-k_z^2}} \left[|\psi_{q\lambda}(z,k_z,k_t)|^2 k_t^2 + |\psi'_{q\lambda}(z,k_z,k_t)|^2\right] dk_t dk_z. \quad (18)$$

In Figure 3, we show the total kinetic density (left panel) and total spin current (right panel) for the Gogny interactions studied in this article. As expected, the spin-current density is strongly localised at the surface of the system and asymptotically goes to 0 since the spin-orbit field vanishes in such a limit. Due to the time-reversal breaking [38], an additional non-local spin orbit field $W_q(z,z')$ should also be considered, but according to the numerical tests done in Ref. [17], such a term can be safely neglected in order to simplify our task.

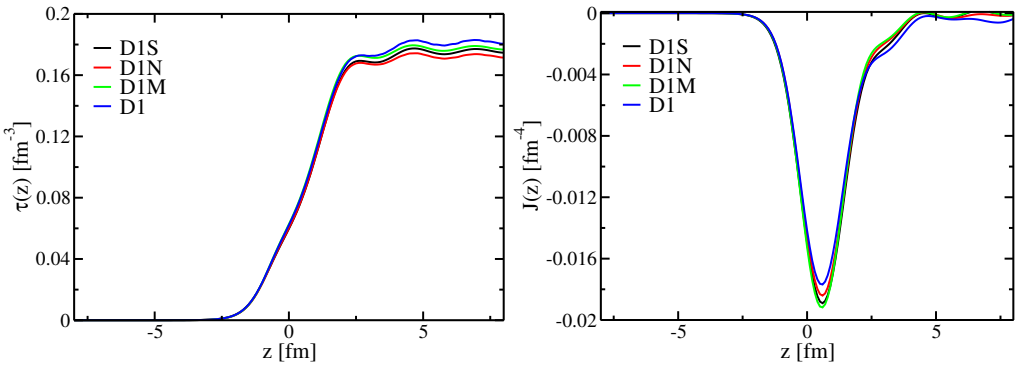

Figure 3. Total kinetic and spin-current density profile for various Gogny interactions calculated in SINM at $\beta = 0$. See text for details.

By solving Equation (12) via the numerical procedure detailed in Section 3.1, we can calculate the total energy density of the system as

$$\mathcal{E}(z) = \frac{1}{2}\sum_q \left\{\varepsilon_q(z) + \frac{\hbar^2}{2m}\tau_q(z)\right\} - U_{rearr}(z)\rho(z) \quad (19)$$

where

$$\varepsilon_q(z) = \frac{1}{\pi^2}\sum_\lambda \int_0^{k_{Fq}} \int_0^{\sqrt{k_{Fq}^2-k_z^2}} \varepsilon_{q\lambda}(k_z,k_t)|\psi_{q\lambda}(z,k_z,k_t)|^2 k_t dk_t dk_z \quad (20)$$

$$U_{\rm rearr}(z) = \alpha t_3 \rho(z)^{\alpha-1}\left[\frac{1}{2}\left(1+\frac{x_3}{2}\right)\rho(z)^2 - \frac{1}{4}(1+2x_3)\sum_q \rho_q(z)^2\right] \quad (21)$$

$U_{\rm rearr}(z)$ is a rearrangement term arising from the explicit density dependence of the Gogny interaction [1]. Finally, Equation (19) together with Equation (16) allows us to calculate the surface energy of the system using Equation (9).

In the previous derivation, we have explicitly neglected the effects arising from the presence of a residual pairing interaction. Previous studies [39,40] have shown that the pairing field is peaked at the surface of SINM; we thus may expect that it could have an impact on the diffusivity of the density and thus on the values of the surface energy. An accurate study would require us to describe the system using Hartree–Fock–Bogoliubov (HFB) equations [1]. Since the pairing field has a smaller magnitude than the central and spin-orbit fields, we may assume that the error we introduce by using HF instead of HFB is quite small.

3. Results

3.1. Numerical Procedure

The most natural way to solve Equation (12) is to use the Numerov method [41]. To this purpose, we express the single particle wave function in the two asymptotic regions along the z axis

$$\lim_{z\to\pm\infty}\psi_{q\lambda}(z,k_z,k_t)=\begin{cases}\sin\big(k_z z+\delta_{q\lambda}(k_z,k_t)\big)\\ A_{q\lambda}(k_z,k_t)\exp\big[-\gamma_q(k_z,k_t)z\big].\end{cases} \tag{22}$$

Using these expressions at the edge of the box L, we can propagate backward (forward) the solutions using the Numerov algorithm [2] and identify both the constant $A_{q\lambda}$ and the phase shift $\delta_{q\lambda}$ using a matching procedure [42] for a given value of the pair of momenta k_z, k_t for fixed λ and q. The quantity $\gamma_q(k_z,k_t)$ is fixed as

$$\gamma_q(k_z,k_t)=\sqrt{k_t^2-\frac{2m}{\hbar^2}\varepsilon_q(k_z,k_t)}. \tag{23}$$

Since the system is infinite along the z direction, the bulk region is not affected by the presence of a surface, and as such, the single particle energies $\varepsilon_q(k_z,k_t)$ are exactly the same that one obtains when solving the HF equations in INM. They read

$$\varepsilon_q(k_z,k_t)=\frac{\hbar^2}{2m}(k_z^2+k_t^2)+U_q^\infty(\sqrt{k_z^2+k_t^2}) \tag{24}$$

where $U_q^\infty(\sqrt{k_z^2+k_t^2})$ corresponds to the HF potential in the infinite medium and represents the limit for $z\to+\infty$ of the combined HF potentials given in Equations (13) and (14). The analytical expression of $U_q^\infty(k)$ is given in Appendix A.

A detailed discussion about the numerical issues related to the solution of this system for zero-range interactions can be found in Ref. [43]. Although the Numerov method is also suitable for differential equations having a source term as in Equation (12), we find that it is numerically more stable to use the trick suggested in Ref. [44], i.e., to transform the source term in Equation (12) to a locally equivalent potential by multiplying and dividing by the wavefunction. In order to avoid infinities in the formula, we used the modification introduced in Ref. [45], so our modified HF equations now read

$$\begin{aligned}\left(-\frac{\hbar^2}{2m}\frac{d^2}{dz^2}+V_{q\lambda}^{loc}(z,k_z,k_t)+\lambda k_t W_q^0(z)-\varepsilon_q+\frac{\hbar^2k_t^2}{2m}\right)\psi_{q\lambda}(z,k_z,k_t)\\ =F_{q\lambda}(z,k_z,k_t)\int_{-\infty}^{\infty}U_q^1(z,z',k_t,k_z)\psi_{q\lambda}(z',k_z,k_t)dz'\end{aligned} \tag{25}$$

where

$$V_{q\lambda}^{loc}(z,k_z,k_t) = U_q^0(z) - \frac{1-F_{q\lambda}(z)}{\psi_{q\lambda}^{bef}(z,k_z,k_t)} \int_{-\infty}^{\infty} U_q^1(z,z',k_t,k_z)\psi_{q\lambda}(z',k_z,k_t)dz' \tag{26}$$

The function $F_{q\lambda}(z,k_z,k_t)$ is defined as

$$F_{q\lambda}(z,k_z,k_t) = \exp\left(-100\left|\frac{\psi_{q\lambda}^{\rm bef}(z,k_z,k_t)}{(\psi_{q\lambda}^{\rm bef})'(z,k_z,k_t)}\right|^2\right) \tag{27}$$

As discussed in Ref. [45], the use of this function avoids the local potential going to infinity in the proximity of a node of the wavefunction. See also discussion in Ref. [46] for more details.

Since the Fock potential depends on the solution $\psi_{q\lambda}(z,k_z,k_t)$, we perform a series of iterations where we freeze the potential, and we solve the HF equations iteratively. To avoid numerical noise, we found that it is advantageous to use for the first iteration of this procedure the single particle wavefunctions of an infinite step-like potential in the z direction, whose solutions are analytical. We thus use such a guess to calculate the integral of the Fock field in Equation (25), and we use the Numerov algorithm to solve Equation (25). We thus obtain a wavefunction that is typically different from the one we used as a guess, so we calculate the integral of the Fock term again and we solve another time Equation (25). This procedure is performed n times until the wavefunctions of the iteration $n-1$ are similar to the ones obtained in the current iteration up to an accuracy parameter

$$\delta = \int_{-L}^{L} \left|\psi_{q\lambda}^{n-1}(z,k_z,k_t) - \psi_{q\lambda}^{n}(z,k_z,k_t)\right| dz \leq 10^{-10}\text{fm}^{1/2} \;\; \forall\, q,\lambda,k_z,k_t\,, \tag{28}$$

In Ref. [17], these are called *minor iterations*. The superscript 'bef' on the wavefunction labels the wavefunction obtained in the minor iteration $n-1$.

Finally, once we observe that we recalculate the new fields. This represents the *major iterations*, now labelled j, and we iterate until the variation (in absolute value) of the relative total energy of the system

$$\delta E = \left|\frac{E_L^{j-1} - E_L^j}{E_L^j}\right|, \tag{29}$$

is less than an accuracy parameter $\delta E \leq 10^{-8}$ MeV. In this way, one introduces an uncertainty of the order of the eV on the surface energy, which is clearly negligible for the purpose of this study.

Other methods have been developed to solve HF equations using non-local potentials [47], but we found the current implementation on two nested loops quite fast since after the first few major iterations, the shape of the wavefunctions tends to stabilise and thus require less and less minor iterations in order to converge.

The integrals in k_z, k_t appearing, for example, in Equation (14) have been performed numerically using Simpson's rule [48] using 30 points for k_z and 12 points for k_t. As discussed in Ref. [17], the integration over k_z requires more accuracy than the one on k_t. The values we used, together with the choice of the box, allow us to obtain results that are numerically stable.

3.2. Surface Energy

In practice, we have to impose a limit on the size of the slab to perform the numerical calculation. This limit is governed by the presence of Friedel oscillations whose typical length scale L_F is of order $\pi/k_F \simeq 2.3$ fm at saturation density. To extract a reliable value of a_s, we thus considered $L \gg L_F$ fm and checked that our results (see Table 2) are not

sensitive to L. For sake of completeness, the results provided in Table 2 have been obtained using $L = 9$ fm.

Table 2. Surface energy coefficient for various Gogny interactions. See text for details.

	a_s [MeV]
D1	20.3
D1S	18.4
D1N	18.2
D1M	18.5

D1 excepted, we found that the existing standard parametrisations of Gogny interactions have surface energy coefficients around 18.3 ± 0.2 MeV. The results presented here are in good agreement with the one of Ref. [17], given the uncertainties related to the employed numerical methods [14].

4. Conclusions

In this paper, we have performed Hartree–Fock calculations in semi-infinite nuclear matter and extended the pioneering results obtained by J. Côté and M. Pearson for D1 to other standard Gogny interactions. Extensions to interactions such as D1P and D2 are under study.

This work takes place in the more general context of obtaining modern parametrisations, which include directly in the fitting protocol more physical constraints. In such a framework, this work will be used in the very near future to compare the results presented here with a semi-classical approach, that is, an analytical formula that can be incorporated into a fitting procedure.

Author Contributions: Conceptualization, D.D., A.P. and J.N.; Methodology, D.D., A.P. and J.N.; Investigation, D.D., A.P. and J.N; Writing—original draft, D.D., A.P. and J.N. All authors have read and agreed to the published version of the manuscript.

Funding: This research received no external funding.

Data Availability Statement: All data required to reproduced the results presented here are available in published papers.

Acknowledgments: The authors would like to thank J. Côté and M. Pearson for very fruitful exchanges about their calculations and the numerical procedures they adopted to solve HF equations.

Conflicts of Interest: The authors declare no conflict of interest.

Appendix A. Gogny Potential in INM

The expression for the potential $U_q^\infty(k)$ reads

$$\begin{aligned} U_q^\infty(k) &= \sum_i \Big[A_0^i \rho + \tau A_1^i \rho\beta + B_{nn}^i u(\mu_i k, \mu_i k_F^q) + B_{np}^i u(\mu_i k, \mu_i k_F^{-q}) \Big] \\ &+ \frac{3}{4} t_3 \rho^{\alpha+1} - \tau \frac{1}{4} t_3 (1 + 2x_3) \rho^{\alpha+2} \beta \,, \end{aligned} \tag{A1}$$

where

$$A_0^i = \frac{\pi^{3/2}\mu_i^3}{4}(4W_i + 2B_i - 2H_i - M_i)\,, \tag{A2}$$

$$A_1^i = \frac{\pi^{3/2}\mu_i^3}{4}(-2H_i - M_i)\,, \tag{A3}$$

$$B_{nn}^i = -\frac{1}{\sqrt{\pi}}(W_i + 2B_i - H_i - 2M_i)\,, \tag{A4}$$

$$B_{np}^i = \frac{1}{\sqrt{\pi}}(H_i + 2M_i)\,, \tag{A5}$$

and takes the value $\tau = +1(-1)$ for neutrons (protons). We also used $\beta = \frac{\rho_n - \rho_p}{\rho_0}$. The function $u(x,y)$ is defined as

$$u(x,y) = \frac{1}{x}\left[e^{-\frac{(x+y)^2}{4}} - e^{-\frac{(x-y)^2}{4}}\right] + \frac{\sqrt{\pi}}{2}\left[\mathrm{erf}\left(\frac{x+y}{2}\right) - \mathrm{erf}\left(\frac{x-y}{2}\right)\right] \tag{A6}$$

here erf(t) is the error function [37]. A similar expression was already given in Ref. [49].

Notes

[1] Notice there is a typo in Equation (3).26 of Ref. [17]

[2] In order to apply the Numerov method, we use a step of 0.1 fm along the z direction

References

1. Ring, P.; Schuck, P. *The Nuclear Many-Body Problem*; Springer: Berlin/Heidelberg, Germany, 1980.
2. Pastore, A. An introduction to bootstrap for nuclear physics. *J. Phys. G Nucl. Part. Phys.* **2019**, *46*, 052001. [CrossRef]
3. Brink, D.M.; Broglia, R.A. *Nuclear Superfluidity: Pairing in Finite Systems*; Cambridge University Press: Cambridge, UK, 2005; Volume 24.
4. Bender, M.; Heenen, P.H.; Reinhard, P.G. Self-consistent mean-field models for nuclear structure. *Rev. Mod. Phys.* **2003**, *75*, 121–180. [CrossRef]
5. Vautherin, D.; Brink, D.M. Hartree-Fock calculations with Skyrme's interaction. I. Spherical nuclei. *Phys. Rev. C* **1972**, *5*, 626. [CrossRef]
6. Goriely, S.; Tondeur, F.; Pearson, J. A Hartree–Fock nuclear mass table. *At. Data Nucl. Data Tables* **2001**, *77*, 311–381. [CrossRef]
7. Skyrme, T. The effective nuclear potential. *Nucl. Phys.* **1958**, *9*, 615–634. [CrossRef]
8. Dechargé, J.; Gogny, D. Hartree-Fock-Bogolyubov calculations with the D1 effective interaction on spherical nuclei. *Phys. Rev. C* **1980**, *21*, 1568. [CrossRef]
9. Nakada, H. Hartree-Fock approach to nuclear matter and finite nuclei with M3Y-type nucleon-nucleon interactions. *Phys. Rev. C* **2003**, *68*, 014316. [CrossRef]
10. Davesne, D.; Becker, P.; Pastore, A.; Navarro, J. Infinite matter properties and zero-range limit of non-relativistic finite-range interactions. *Ann. Phys.* **2016**, *375*, 288–312. [CrossRef]
11. Kortelainen, M.; Lesinski, T.; Moré, J.; Nazarewicz, W.; Sarich, J.; Schunck, N.; Stoitsov, M.; Wild, S. Nuclear energy density optimization. *Phys. Rev. C* **2010**, *82*, 024313. [CrossRef]
12. Chabanat, E.; Bonche, P.; Haensel, P.; Meyer, J.; Schaeffer, R. A Skyrme parametrization from subnuclear to neutron star densities Part II. Nuclei far from stabilities. *Nucl. Phys. A* **1998**, *635*, 231–256. [CrossRef]
13. Erler, J.; Klüpfel, P.; Reinhard, P. Misfits in Skyrme–Hartree–Fock. *J. Phys. G Nucl. Part. Phys.* **2010**, *37*, 064001. [CrossRef]
14. Jodon, R.; Bender, M.; Bennaceur, K.; Meyer, J. Constraining the surface properties of effective Skyrme interactions. *Phys. Rev. C* **2016**, *94*, 024335. [CrossRef]
15. Ryssens, W.; Bender, M.; Bennaceur, K.; Heenen, P.H.; Meyer, J. Impact of the surface energy coefficient on the deformation properties of atomic nuclei as predicted by Skyrme energy density functionals. *Phys. Rev. C* **2019**, *99*, 044315. [CrossRef]
16. Proust, P.; Lallouet, Y.; Davesne, D.; Meyer, J. Surface energy coefficient of an N2LO Skyrme energy functional: A semiclassical extended Thomas-Fermi approach. *Phys. Rev. C* **2022**, *106*, 054321. [CrossRef]
17. Côté, J.; Pearson, J. Hartree-fock calculations of semi-infinite nuclear matter with complete forces (finite-range and spin-orbit term). *Nucl. Phys. A* **1978**, *304*, 104–126. [CrossRef]
18. Chamel, N.; Haensel, P. Physics of neutron star crusts. *Living Rev. Relativ.* **2008**, *11*, 10. [CrossRef]
19. Davesne, D.; Pastore, A.; Navarro, J. Linear response theory with finite-range interactions. *Prog. Part. Nucl. Phys.* **2021**, *120*, 103870. [CrossRef]

20. Farine, M.; Von-Eiff, D.; Schuck, P.; Berger, J.; Dechargé, J.; Girod, M. Towards a new effective interaction of the Gogny type. *J. Phys. G Nucl. Part. Phys.* **1999**, *25*, 863. [CrossRef]
21. Grasso, M.; Anguiano, M. Tensor parameters in Skyrme and Gogny effective interactions: Trends from a ground-state-focused study. *Phys. Rev. C* **2013**, *88*, 054328. [CrossRef]
22. Otsuka, T.; Matsuo, T.; Abe, D. Mean field with tensor force and shell structure of exotic nuclei. *Phys. Rev. Lett.* **2006**, *97*, 162501. [CrossRef]
23. Chappert, F.; Pillet, N.; Girod, M.; Berger, J.F. Gogny force with a finite-range density dependence. *Phys. Rev. C* **2015**, *91*, 034312. [CrossRef]
24. Berger, J.; Girod, M.; Gogny, D. Microscopic analysis of collective dynamics in low energy fission. *Nucl. Phys. A* **1984**, *428*, 23–36. [CrossRef]
25. Dutra, M.; Lourenço, O.; Martins, J.S.; Delfino, A.; Stone, J.R.; Stevenson, P. Skyrme interaction and nuclear matter constraints. *Phys. Rev. C* **2012**, *85*, 035201. [CrossRef]
26. Centelles, M.; Roca-Maza, X.; Vinas, X.; Warda, M. Nuclear symmetry energy probed by neutron skin thickness of nuclei. *Phys. Rev. Lett.* **2009**, *102*, 122502. [CrossRef] [PubMed]
27. Roca-Maza, X.; Centelles, M.; Vinas, X.; Warda, M. Neutron skin of Pb 208, nuclear symmetry energy, and the parity radius experiment. *Phys. Rev. Lett.* **2011**, *106*, 252501. [CrossRef] [PubMed]
28. Fattoyev, F.; Piekarewicz, J.; Horowitz, C.J. Neutron skins and neutron stars in the multimessenger era. *Phys. Rev. Lett.* **2018**, *120*, 172702. [CrossRef] [PubMed]
29. Reed, B.T.; Fattoyev, F.J.; Horowitz, C.J.; Piekarewicz, J. Implications of PREX-2 on the equation of state of neutron-rich matter. *Phys. Rev. Lett.* **2021**, *126*, 172503. [CrossRef]
30. Chappert, F.; Girod, M.; Hilaire, S. Towards a new Gogny force parameterization: Impact of the neutron matter equation of state. *Phys. Lett. B* **2008**, *668*, 420–424. [CrossRef]
31. Goriely, S.; Hilaire, S.; Girod, M.; Péru, S. First Gogny-Hartree-Fock-Bogoliubov nuclear mass model. *Phys. Rev. Lett.* **2009**, *102*, 242501. [CrossRef]
32. Libert, J.; Girod, M.; Delaroche, J.P. Microscopic descriptions of superdeformed bands with the Gogny force: Configuration mixing calculations in the A 190 mass region. *Phys. Rev. C* **1999**, *60*, 054301. [CrossRef]
33. Sobiczewski, A.; Litvinov, Y.A. Predictive power of nuclear-mass models. *Phys. Rev. C* **2014**, *90*, 017302. [CrossRef]
34. Swiatecki, W. The nuclear surface energy. *Proc. Phys. Soc. Sect. A* **1951**, *64*, 226. [CrossRef]
35. Friedel, J. Metallic alloys. *Nuovo Cim. (1955–1965)* **1958**, *7*, 287–311. [CrossRef]
36. Stocker, W. Spin-orbit coupling and properties of the nuclear surface. *Nucl. Phys. A* **1970**, *140*, 305–318. [CrossRef]
37. Abramowitz, M.; Stegun, I.A.; Romer, R.H. Handbook of mathematical functions with formulas, graphs, and mathematical tables. *Am. J. Phys.* **1988**, *56*, 958. [CrossRef]
38. Rohoziński, S.; Dobaczewski, J.; Nazarewicz, W. Self-consistent symmetries in the proton-neutron Hartree-Fock-Bogoliubov approach. *Phys. Rev. C* **2010**, *81*, 014313. [CrossRef]
39. Baldo, M.; Lombardo, U.; Saperstein, E.; Zverev, M. Microscopic study of the effective pairing interaction in semi-infinite nuclear matter with the separable NN-interaction. *Nucl. Phys. A* **1998**, *628*, 503–536. [CrossRef]
40. Baldo, M.; Lombardo, U.; Saperstein, E.; Zverev, M. Solving the Bogolyubov equations for semi-infinite nuclear matter in the case of a nonlocal gap. *Phys. At. Nucl.* **1999**, *62*, 66–85.
41. Noumerov, B. A method of extrapolation of perturbations. *MNRAS* **1924**, *84*, 592. [CrossRef]
42. Bennaceur, K.; Dobaczewski, J. Coordinate-space solution of the Skyrme–Hartree–Fock–Bogolyubov equations within spherical symmetry. The program HFBRAD (v1. 00). *Comput. Phys. Commun.* **2005**, *168*, 96–122. [CrossRef]
43. Bonche, P.; Koonin, S.; Negele, J. One-dimensional nuclear dynamics in the time-dependent Hartree-Fock approximation. *Phys. Rev. C* **1976**, *13*, 1226. [CrossRef]
44. Vautherin, D.; Vénéroni, M. Solution of the nuclear Hartree-Fock equations in coordinate space. *Phys. Lett. B* **1967**, *25*, 175–178. [CrossRef]
45. Michel, N. A simple and efficient numerical scheme to integrate non-local potentials. *Eur. Phys. J. A* **2009**, *42*, 523–527. [CrossRef]
46. Grasso, M.; Van Giai, N.; Sandulescu, N. Continuum HFB calculations with finite range pairing interactions. *Phys. Lett. B* **2002**, *535*, 103–108. [CrossRef]
47. Blanchon, G.; Dupuis, M.; Arellano, H.F.; Bernard, R.; Morillon, B. SIDES: Nucleon–nucleus elastic scattering code for nonlocal potential. *Comput. Phys. Commun.* **2020**, *254*, 107340. [CrossRef]
48. Atkinson, K.E. *An Introduction to Numerical Analysis*; John Wiley and Sons: New York, NY, USA, 1989.
49. Sellahewa, R.; Rios, A. Isovector properties of the Gogny interaction. *Phys. Rev. C* **2014**, *90*, 054327. [CrossRef]